# Angular Distribution of the $(d,p)$ Reactions Making Two Low States of $O^{17}$

N. P. HEYDENBURG
*Department of Terrestrial Magnetism of The Carnegie Institution of Washington, Washington, D. C.*

AND

D. R. INGLIS
*Department of Physics, The Johns Hopkins University, Baltimore, Maryland*

(Received October 27, 1947)

Angular distributions of the protons from deuteron bombardment of fairly thin oxide targets have been observed both for the long-range protons leading to the ground state of the residual nucleus $O^{17}$, and for the short-range protons leading to the first excited state. The deuteron energies ranged from 0.65 to 3.05 Mev, and the beam, obtained at each energy from one of two statitrons, was practically monoenergetic. The protons were observed by an ionization chamber, linear amplifier, and pulse height discriminator, while the monitoring was done by integrating target current. The yield of the short-range protons is about ten times that of the long-range protons at low bombarding energies, and the two yields become nearly equal at higher energies. Very pronounced variation of proton intensity with angle was observed for both ranges at almost all bombarding energies, the shape of the curves varying markedly with energy. At low bombarding energies the long-range protons are predominantly forward, the short-range predominantly backward. In the neighborhood of a peak in the excitation curves at about 1.8 Mev, the angular distributions become roughly symmetric about 90° for both ranges, and even almost isotropic for the long-range protons. It happens that the high energy side of this peak coincides rather closely with the threshold of the competing $(d,n)$ reaction. This peak appears for both ranges in the excitation curves for the total yield, integrated over all angles, but not in the conventional 90° excitation curves. Two further peaks appear at higher energies. It is hoped that relationships between the angular momentum properties of the two low states of the final nucleus may be deduced from detailed angular information of the sort here presented.

KNOWLEDGE of the low states of the simpler light nuclei gives particular promise of being helpful in leading to an understanding of nuclear structure. Acquaintance with the properties of more than one state in a single nucleus might be expected to contribute to the problem in a manner somewhat analogous to that in which spectroscopic information on many levels of simpler atoms helped unravel the problem of atomic structure. The $O^{17}$ nucleus is probably an unusually simple one when not too highly excited because the stability of the $O^{16}$ nucleus and its "completed-shell" nature in either the central or the alpha model makes it likely that the low states of $O^{17}$ may be better approximated by a single-particle model than may those of most nuclei. The experimental investigation here reported was motivated by the hope that it might make possible a comparison of the angular properties of the two low states of $O^{17}$. (The present state of the analysis is not such that this hope is realized.)

The two ranges of the protons from the $O^{16}(d,p)O^{17}$ reaction have been observed by Cockroft and Lewis[1] at right angles to their incident deuteron beam, which had an energy of 575 kev. The two ranges were resolved as rather sharp peaks, at about 4-cm and 8-cm air equivalent. The short-range peak was about $2\frac{1}{2}$ times as high as the long-range peak.

In the first phase of the present experiments, deuteron energies were used up to 1150 kev, this being the highest energy available from the small statitron at D.T.M. This atmospheric-pressure machine was selected as the one which could be put into operation most quickly after the recent prolonged hiatus in research activities. During the course of the investigation, the voltage control of this statitron has been improved by installation of equipment which utilizes the "voltmeter current," taken from the high voltage head through a $10^{10}$-ohm resistor stack,[2] to control the corona current[3] allowed to leak from a corona arm back to the head. The behavior of the resistor stack was improved by installing more closely spaced shielding rings and corona points outside the textolite casing. The voltage regulation achieved is better than one-half percent although the calibration may

[1] J. D. Cockroft and W. B. Lewis, Proc. Roy. Soc. **154**, 250 (1936).

[2] M. A. Tuve Sci. Month. **47**, 4, p. 8 (1938).

[3] A. O. Hanson, Rev. Sci. Inst. **15**, 60 (1944).

gradually drift more than this because of temperature changes.

Toward the end of the first phase of the work, trouble developed in the ion source power supply of the small statitron which made necessary the start of some rebuilding at the completion of this phase. At about this time the large statitron[4] was brought into operating condition, and the second phase of the work consisted of carrying the measurements up to bombarding energies of 3 Mev with this machine. Modifications and improvements in this statitron which helped bring it into operating condition included the building of a new electrostatic voltmeter, the installation of a new set of fixed corona points and shunting sphere gaps, the installation of a system of variable corona gaps between the platforms at four-foot intervals up the supporting column, and the use of a rather soft mixture of "W" wax and "J" oil on the joints in the accelerating tube, where cracks had been developing in ordinary "W" wax during the cold weather of the winter. Lacking a voltmeter stack or electrostatic deflector, the voltage regulation is carried out on the large statitron by manual adjustment of the charging current, according to indications of the oscilloscope trace obtained from the generating voltmeter. The regulation of bombarding voltage was always good to about 1 percent, and under the most favorable conditions to better than $\frac{1}{4}$ percent.

## EXPERIMENTAL ARRANGEMENT

### Target Chamber

The target chamber found most satisfactory for measuring the angular distribution of the protons produced by the $O^{16}(d,p)O^{17}$ reaction is shown in Fig. 1. The chamber itself is the same one that was used earlier[5] at the Johns Hopkins Physics Department for the observation of alphas resulting from the proton bombardments, but the method of observing the product particles is quite different in the present work. The chamber had windows allowing observation at five angles, and more were added toward the end of this work. An ionization chamber and pre-preamplifier are mounted on a screw-adjusted, radially traveling carriage which in turn is mounted on a swivel arm screwed to one face of the chamber, the pivot bolt being at the center of the face. A graduated circle is mounted around the edge of this face, so that the angular position of the swivel arm may be read. With the angular position adjusted to suit one of the windows, the distribution of the protons in

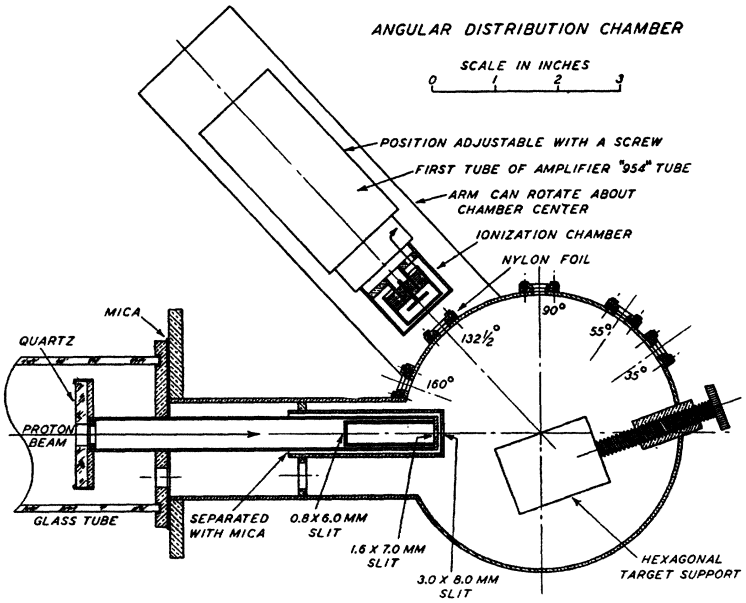


FIG. 1. Target chamber.

[4] Reference 2, p. 19.
[5] Swartz, Rossi, Jennings, and Inglis, Phys. Rev. 65, 80 (1944).

range is investigated by measuring the frequency of proton counts as dependent on the radial position of the carriage. Thus air at atmospheric pressure is used as the variable absorber. The discriminator bias is set at such a value that only those particles having the ends of their ranges near the back of the ionization chamber are counted.

The first of these experiments with this chamber were carried out with 0.0005-inch aluminum windows, but difficulties were experienced especially in variation of the shape of the peaks from one window to another. (The short-range peak was so close to the window that no adequate check could be obtained between the two peaks to make sure that the effect was attributable to the windows.) Some windows gave the appearance of a plateau on the short-range side of the long-range peak, as though perhaps one-third of the area of the window were about twice as thick as the rest. (The nominal thickness of the Al windows was 2-cm air equivalent, and the plateau was displaced about 1 or $1\frac{1}{2}$ cm from the peak). Whatever the origin of these troubles, they vanished with the use of Nylon windows and the improvement of the electronic technique.

The great advantage of Nylon windows is that they are so thin as to make one confident that variations in their thickness cannot lead to appreciable uncertainties in the ranges of the particles. Their nominal thickness is 0.0005 in., which means an air equivalent of about 2 mm. The disadvantage is that they do not last long under particle bombardment. With primary currents of the order of a few tenths of a microampere getting through the slit system to the target, the life of the windows is only three or four hours. The secondary particles being counted amount to only a few dozen per square millimeter per second, but shorter-ranged primary particles scattered from the target are probably responsible for the short window life. It is convenient that the windows give warning by leaking slowly for some time before actually bursting, so that vacuum calamities may usually be avoided.

In the final arrangement used at the lower bombarding energies, each of the five Nylon windows is mounted in a window frame in such a way that its inner side is pressed around the edges against a $\frac{1}{16}$-in.$\times\frac{1}{16}$-in. Neoprene gasket which is sunk in a groove 3/64-in. deep. The lower plate of the window frame is shaped to fit the cylindrical surface of the target chamber, and is pressed against it with a flat ungrooved rubber gasket. The window itself measures 5 mm$\times$9 mm, being rounded toward the ends, and the direction of greatest strength in the Nylon is placed the short way across the window. Windows a couple of millimeters wider did not last as long as an hour.

At the higher bombarding energies the range of the short-range protons was sufficient that duraluminum windows of 6-cm air equivalent could be used and these were nicely homogeneous. Extra stopping foils of the same material were used to shorten the distance from target to counter and increase the counting rate.

The target chamber arrangement first used in this investigation appeared more elegant, but was not very successful because the connection between the collecting electrode and the first grid was so long that the pulses were only slightly higher than the noise level. This chamber had a swivel arm inside the vacuum, pivoting on a conical ground joint (as used formerly at D.T.M. for proton-proton and proton-helium scattering measurements[6]), and carrying a double chamber with two pressure tubes and a high voltage lead in addition to the pulse connection (which came out of the opposite face of the target chamber to the external pre-preamplifier). The first compartment of this double chamber was a variable-pressure absorption cell with an aluminum window at each end, and the second part was the usual ionization chamber.

### Electronic Equipment

The pre-preamplifier which travels on the ionization chamber carriage is a 954 Acorn tube, which has been found consistently superior to other tubes tried for this purpose, now just as several years ago. It is connected by a short flexible connector to a 3-stage preamplifier consisting of three 6AK5 tubes in a negative-feedback loop. This in turn is connected by a longer lead to a rather new linear amplifier ("Model 100" as designed by W. A. Higinbotham for

[6] N. P. Heydenburg, L. R. Hafstad, and M. A. Tuve, Phys. Rev. 56, 1078 (1939).

faster counting than encountered here, with the input slowed down for total ion collection, to eliminate high-frequency noise) and this feeds the pulses into a discriminator and scale-of-eight recorder which has been in use in this laboratory for some time. During the second phase of the work, a discriminator and scale-of-64 of Higinbotham's design replaced the old scale-of-8 and seemed to discriminate just as dependably until the humidity of the summer was accompanied by trouble which was eliminated by a return to the old scalar.

The preliminary observations were made by integrating current over time visually, taking runs for a given time, because current integrators had not been found very accurate in earlier work in this laboratory. During the course of the investigation, two current integrators were built and tried. The first depended on the firing of a thyrotron and did not achieve a reliably functioning condition. The second is a more complicated circuit designed by M. Sands. It has been very satisfactory and has greatly facilitated the final measurements.

## PROCEDURE

The target used for most of the measurements is in effect a fairly thin target of ordinary oxygen, but is actually an oxide layer on a tungsten surface. The tungsten surface was polished with emery cloth and then heated to a dull red glow. During the heating the spreading of successive layers of oxide across the surface could be seen in reflected light, and the target was considered completed when three or four such layers had appeared. The plate was then mounted on a hexagonal copper-block target mounting capable of being rotated from outside the target chamber through a screw which also allows advancement to a fresh target position after a target spot has become contaminated with superposed carbon deposited by the beam.

Alignment to place the target spot at the center of the chamber is aided by the possibility of turning a quartz target in place to make the spot easily visible, but a slight glow can also be seen on the oxide target itself for purposes of more accurate alignment. The possibility of sighting visually through the Nylon windows is also helpful. The most important requirement is that the edges of the windows should not partially eclipse the lines between the edges of the target spot and the edges of the ionization chamber aperture, and this is assured by picking the angle setting suited to each window by means of trial runs with given range settings and varying angle settings.

Some preliminary runs at fixed angle covered a domain of range wide enough to include both the 4-cm and the 8-cm peak and the region between them to verify the observation of Cockroft and Lewis that there are only two peaks in this domain. Subsequently attention was focused only on the peaks themselves. A typical curve showing the appearance of the peaks is shown in Fig. 2. It was taken toward the end of the work with the thin target on steel,

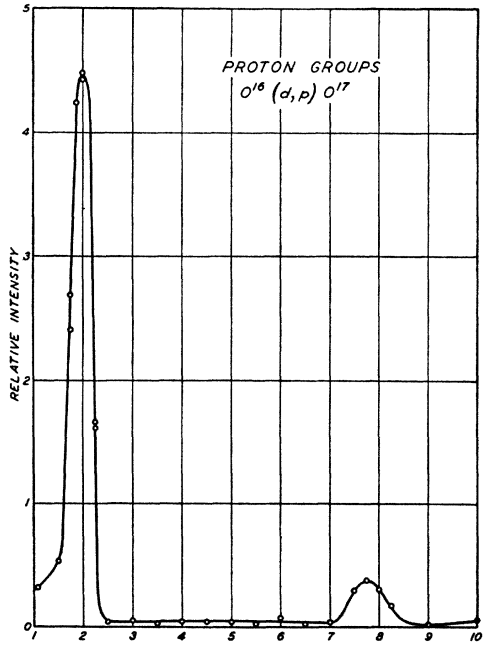


FIG. 2. A typical yield curve as a function of range, showing the appearance of the two groups of protons. This was observed at a bombarding energy of 1.15 Mev and $\theta=90°$. Only the inverse-square correction has been made. To the observed range as plotted should be added the window thickness (5.2-cm air equivalent) and approximately the thickness of the ionization chamber (3 mm). The long-range peak is then at 13.2 and the short-range peak at 7.5 cm. According to Livingston and Bethe's range-energy curve, these correspond to 2.89 and 2.07 Mev. From these data we find the energy evolutions $Q_{l.r.}=2.05\pm0.2$ Mev and $Q_{s.r.}=1.18\pm0.2$ Mev, and the energy of the excited state of $O^{17}$, $Q_{l.r.}-Q_{s.r.}=0.87\pm0.03$ Mev, which while consistently larger, are not in disagreement with the earlier values. From this $Q_{l.r.}$ we obtain $M(O^{17})=17.00908\pm0.0002$.

TABLE I. Intensities in the center-of-mass system at various angles and bombarding energies. The tabulated numbers are the numbers of protons recorded per current-integrator count (0.41$\mu$ coulomb) in a solid angle which would be subtended by the ion chamber aperture (area 0.13 cm²) at 10¼ cm from the target. The angles listed are laboratory angles; for center-of-mass angles see Table II. The energies are laboratory bombarding energies. The target is slightly thick oxide on tungsten except where otherwise noted.

| $E$/Mev | 35° | 55° | 72.5° | 90° | 110° | 132.5° | 160° |
|---|---|---|---|---|---|---|---|
| Short range | | | | | | | |
| 0.650 | 0.30 | 0.22 | | 0.68 | | 1.57 | 1.68 |
| 0.750 | 0.73 | 0.77 | | 2.51 | | 3.86 | 3.72 |
| 0.930* | 2.74 | 4.03 | | 11.56 | | 13.64 | 13.54 |
| 0.933 | 1.97 | 2.89 | | 9.76 | | 10.94 | 11.02 |
| 1.070 | 5.94 | 7.17 | | 15.4 | | 17.6 | 15.72 |
| 1.150 | 7.23 | 8.19 | | 17.8 | | 19.5 | 17.49 |
| 1.52 | 9.58 | 14.5 | | 33.7 | | 33.1 | 22.0 |
| 1.71* | 8.76 | 18.24 | 26.80 | 29.3 | 26.0 | 15.6 | 10.1 |
| 1.785 | 16.65 | 30.9 | | 41.9 | | 22.0 | 4.95 |
| 1.935 | 25.6 | 24.4 | | 27.4 | | 23.2 | 14.3 |
| 2.045 | 40.5 | 19.35 | | 39.2 | | 46.3 | 33.5 |
| 2.34 | 24.7 | 17.85 | | 53.2 | | 34.4 | 20.5 |
| 2.60 | 7.43 | 40.5 | | 39.0 | | 15.5 | 15.8 |
| 3.05 | 16.7 | 33.6 | | 40.2 | | 18.25 | 9.9 |
| 0.80** | 0.66 | 0.51 | | 2.08 | | 2.94 | 2.93 |
| 0.93** | 1.13 | 1.67 | | 4.55 | | 4.46 | 3.91 |
| 1.15** | 0.57 | 1.30 | | 3.34 | | 2.43 | 1.40 |
| 1.62** | 2.32 | 3.85 | 7.15 | 8.74 | 7.54 | 3.86 | 2.98 |
| 1.71** | 3.70 | 5.50 | 7.11 | 7.40 | 5.82 | 2.90 | 2.33 |
| 1.825** | 7.16 | 4.87 | 5.84 | 4.27 | 4.00 | 3.04 | 2.29 |
| 1.945** | 9.60 | 3.24 | 5.26 | 8.16 | 6.94 | 7.10 | 5.98 |
| 2.045** | 9.19 | 2.90 | 7.11 | 10.95 | 11.96 | 11.57 | 8.85 |
| Long range | | | | | | | |
| 0.933 | 2.64 | 3.63 | | 2.40 | | 1.26 | 0.914 |
| 1.070 | 3.99 | 4.96 | | 2.93 | | 1.68 | 1.36 |
| 1.525 | 9.9 | 15.4 | | 12.5 | | 10.84 | 10.25 |
| 1.71* | 57.6 | 90.8 | 89.9 | 88.2 | 100.5 | 132.1 | 156.4 |
| 1.785 | 9.9 | 10.44 | | 10.8 | | 16.6 | 18.8 |
| 2.045 | 10.1 | 14.85 | | 8.88 | | 10.73 | 14.9 |
| 2.34 | 13.85 | 29.7 | | 15.7 | | 18.65 | 29.3 |
| 2.60 | 16.6 | 16.8 | | 15.3 | | 28.5 | 30.9 |
| 3.05 | 32.0 | 45.2 | | 32.05 | | 25.1 | 29.3 |

* Slightly thick oxide on steel.
** Thin oxide on steel.

at 1.15 Mev and 90° (with a bias of 80 volts on the "old" discriminator). The position of course varies with bombarding voltage and with angle in a way which can be calculated from conservation of energy and momentum in the collision. The observed range on the carriage vernier depends further on the amount the Nylon window is bowed in, and this varies from window to window and from run to run just sufficiently that it is considered necessary to take about three readings very close to the expected position of a peak in order to be sure to obtain the height of the peak. This procedure is followed in obtaining curves for the variation of the height of a peak with angle at a given bombarding voltage.

TABLE II. Center-of-mass angles.

| $E$/Mev | 35° | 55° | 72½° | 90° | 110° | 132½° | 160° |
|---|---|---|---|---|---|---|---|
| Short range | | | | | | | |
| 0.65 | 36°40′ | 57°23′ | | 92°54′ | | 134°38′ | 161° |
| 1.0 | 36°53′ | 57°41′ | | 93°17′ | | 134°55′ | 161°7′ |
| 1.5 | 37°5′ | 57°58′ | 75°57′ | 93°37′ | 113°24′ | 135°10′ | 161°14′ |
| 2.0 | 37°12′ | 58°9′ | 76°10′ | 93°51′ | 113°37′ | 135°20′ | 161°19′ |
| 3.0 | 37°22′ | 58°23′ | | 94°8′ | | 135°33′ | 161°25′ |
| Long range | | | | | | | |
| 1.0 | 36°35′ | 57°16′ | | 92°56′ | | 134°32′ | 160°57′ |
| 1.5 | 36°48′ | 57°34′ | 75°30′ | 93°8′ | 112°57′ | 134°49′ | 161°4′ |
| 2.0 | 36°56′ | 57°46′ | 75°44′ | 93°21′ | 113°11′ | 135° | 161°9′ |
| 3.0 | 37°9′ | 58°4′ | | 93°44′ | | 135°15′ | 161°17′ |

Because of gradual drift in the effectiveness of the discriminator bias and in the resistance of the voltmeter resistor or in the comparison potential governing the bombarding voltage, it is desirable to group consecutively measurements of which the comparison is most significant. We are primarily interested in angular dependence of the peak height, and secondarily interested in the variation of this property with bombarding voltage. Most runs were therefore made consecutively over different angles, observing either the short-range or the long-range peak at a given bombarding voltage. During such consecutive runs, observations at different bombarding voltages were made at single angles in order to make possible intercomparison with sets of data obtained on different days and under varying conditions. Finally a 90° excitation curve was made to extend this intercomparison over a broad range of energies.

The discriminator bias is kept at a constant value during all these runs. The value was picked in the first place, as a result of experience with preliminary measurements, in such a way as to give as frequent counts as possible without broadening the lines unduly beyond their inevitable width arising from straggling in range. It is to be noted that the cut-off for settings on the long-range side of the peak arises from most of

TABLE III. Correction factor $g$ = (center of mass intensity)/(lab. intensity).

| $E$/Mev | 35° | 55° | 90° | 132½° | 160° |
|---|---|---|---|---|---|
| Short range | | | | | |
| 0.65 | 0.923 | 0.945 | 1.001 | 1.072 | 1.094 |
| 1.0 | 0.913 | 0.939 | 1.001 | 1.082 | 1.104 |
| 1.5 | 0.906 | 0.933 | 1.001 | 1.091 | 1.130 |
| 2.0 | 0.901 | 0.929 | 1.001 | 1.097 | 1.138 |
| 3.0 | 0.893 | 0.923 | 1.002 | 1.106 | 1.152 |
| Long range | | | | | |
| 1.0 | 0.926 | 0.948 | 1.001 | 1.071 | 1.089 |
| 1.5 | 0.918 | 0.941 | 1.000 | 1.068 | 1.110 |
| 2.0 | 0.912 | 0.936 | 1.000 | 1.081 | 1.119 |
| 3.0 | 0.902 | 0.930 | 1.001 | 1.094 | 1.137 |

the particles ending their paths after passing only part way across the chamber, whereas the cut-off on the short-range side arises from most of the particles spending the last and most highly ionizing part of their paths beyond the chamber. If there were no straggling and the bias were set to accept pulses considerably below the maximum, one could obtain a quite unsymmetrical peak from the difference in these two mechanisms of cut-off. The lack of marked asymmetry may be considered some evidence for the reasonableness of the bias setting.

The results as observed in the laboratory coordinate system are transformed to the center-of-mass coordinate system by use of the relation

$$\sin(\theta_r-\theta)=(V/v_r)\sin\theta, \quad (1)$$

and by multiplying the observed relative intensities by the factor which relates the solid angle defined by the ionization chamber aperture in the two systems[7] (see Table III):

$$g(\theta)=\sin\theta d\theta/\sin\theta_r d\theta_r$$
$$=(\sin^2\theta/\sin^2\theta_r)\cos(\theta_r-\theta). \quad (2)$$

The last substitution arises from differentiating (1) with respect to $\theta_r$ and solving for $d\theta/d\theta_r$. In order to find $\theta_r$, the deflection angle in the c.m. system, from (1), the factor $V/v_r$ is computed from the relation

$$(V/v_r)^2=(m_1m_2/m_0m_3)/(1+MQ/m_0E_1) \quad (3)$$

which is obtained from the kinetic energy of the center-of-mass motion,

$$E_{\text{c.m.}}=(1/2)MV^2=(m_1/M)E_1$$

where $M$ is the total mass and $V$ the speed of the center of mass, and from the expression for the kinetic energy after the reaction, relative to the center of mass:

$$E_{\text{rel.}}=(1/2)m_2^2v_r^2(1/m_2+1/m_3)$$
$$=E_1+Q-E_{\text{c.m.}}=(m_0/M)E_1+Q.$$

Here the subscripts 0, 1, 2, and 3 refer to the target nucleus ($O^{16}$), the incident particle (deuteron), the product particle (proton), and the residual nucleus ($O^{17}$), respectively. The variation of $\theta_r$ and $g$ with $\theta$ and $E$ are shown in Table II, in a form convenient for interpolation.

[7] Haxby, Allen, and Williams, Phys. Rev. **55**, 142 (1939).

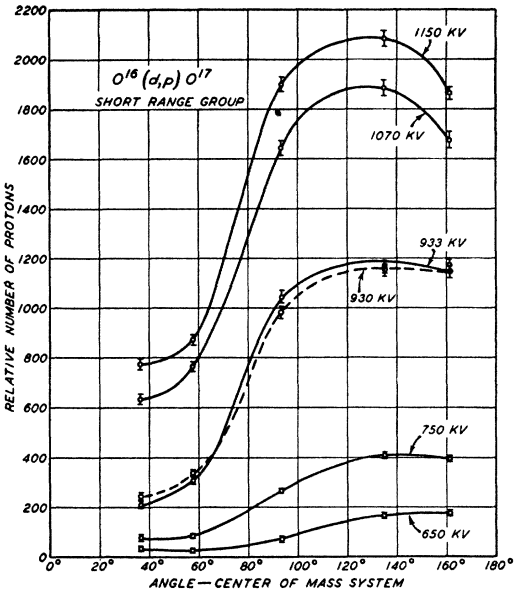


FIG. 3. Angular distributions at low bombarding energies. The solid curves were observed with the small statitron and a slightly thick oxide target on tungsten. The dotted curve was observed later with the large statitron and a slightly thick oxide target on steel.

The expansions in terms of the small quantity $V/v_r$,

$$\theta_r=\theta+(V/v_r)\sin\theta+(1/6)(V/v_r)^3\sin^3\theta+\cdots,$$

$$g(E,\theta)=1-2(V/v_r)\cot\theta$$
$$+(V/v_r)^2(3\cot^2\theta+\tfrac{1}{2})+\cdots,$$

are also sometimes useful. The last term given may usually be neglected.

## RESULTS AND DISCUSSION OF TARGET THICKNESS

In making numerous observations like these it is desirable to strike a compromise between ideal thinness of a target and the demands of intensity. When the original target used in most of the observations was made by oxidizing tungsten to a thickness of about two wavelengths of yellow light, it was not realized that it was anything but ideally thin and no attempt was then made to seek a more appropriate metal. The only criterion used was that the lines seemed to have a width of the order of magnitude of that expected from straggling, and a satisfactory intensity. It turns out that this target is a little thicker than ideal, but the results obtained with it serve to give a good general

view of the variation of angular distribution with energy and are trustworthy except for some slight details. These results transferred to the center-of-mass coordinate system are shown in Figs. 3 and 4. They are also tabulated, along with more recent results, in Table I. The angular distributions shown in Fig. 3, for bombarding energies below 1.15 Mev, were obtained with the small statitron. In this region of energy it seems from these results that there is very little change in the shape of the curves with energy, but only an increase of over-all intensity with energy. The long-range group is predominantly forward and the much more intense short-range group predominantly backward. The results shown in Fig. 4 cover a larger range of bombarding energies and show that the appearance of the angular distributions undergoes wild fluctuations as the energy increases, while the over-all intensity of the long-range group becomes more nearly equal to that of the short-range group. There is a slight semblance of waves of intensity starting at the backward angles and moving forward as the energy is increased.

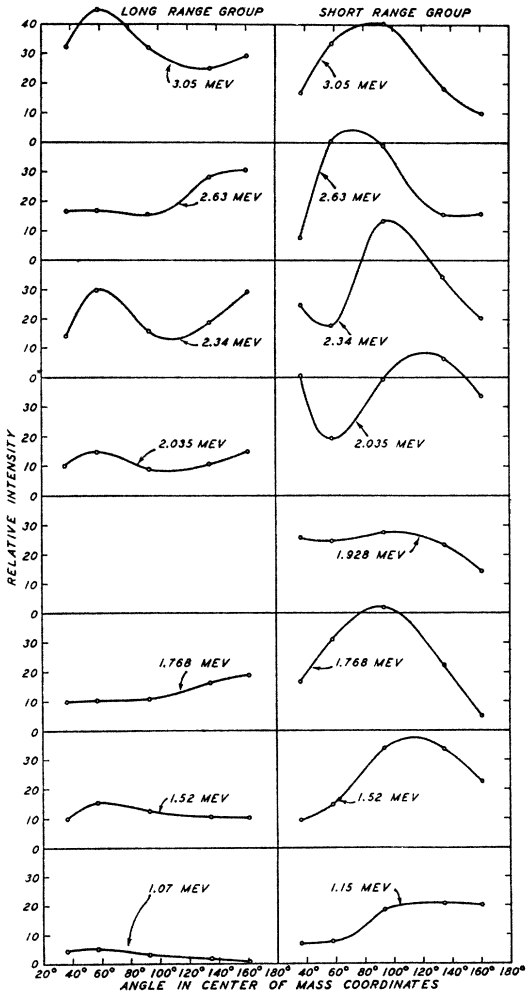


FIG. 4. General trends of the angular distributions over a wide range of energy. Slightly thick oxide targets were used.

The angle of incidence on the target is $22\frac{1}{2}°$, and the most nearly forward angle at which observations were made is 35°, at which position the angle of emergence is as little as $12\frac{1}{2}°$, nearly enough grazing that an appreciable part of the bombarded target area might be eclipsed if the target were microscopically uneven. Such an effect would falsify the angular distribution. To investigate this point, a polished mirror-like steel surface was prepared and oxidized to a dull blue by heating, with the intention to compare results from this with those obtained with the tungsten oxide surface on which most of the observations were made. It was found that this was not really a thin target: the peak width at the 35° position was about twice that at 90°, which latter was about the same as with the tungsten oxide target. (At 1.71 Mev, the short-range peak had a width at half-maximum of 1.2 cm at 90°, 2.4 cm at 35°.) In a repetition of this control experiment, the polished steel was oxidized more lightly, to a very faint bluish tinge, and this oxide layer gave evidence of being thin. The yield with the thin target on steel was about one-fourth that on the slightly too thick layer on steel, and the latter was about the same as that on tungsten in this respect. Observations made with this target are shown in Fig. 5, and also in Table I. These are considered more reliable than the other angular distributions.

## ANALYSIS OF THE RESULTS IN ANGLE FUNCTIONS

The theory of the phenomenon here observed is beyond the scope of this paper. We confine ourselves to a few remarks about the formal analysis of the angular distributions in terms of angle functions, for the sake of preliminary orientation toward the theoretical problem. One of the most striking features of the results is the fact that, over a range of low bombarding

energies, the long-range group is preponderantly backward (with a considerable similarity between the one curve and the mirror image of the other). This is probably to be interpreted as arising from constructive and destructive interference of outgoing $s$ and $p$ waves, the phase relation between the $s$ and $p$ waves being different in the short-range and long-range transition.

Unless there be some unexpected selection rule (such as the failure of spin and orbital angular momenta to be mixed in the reaction), one would expect the observed intensity to be the superposition of several intensities each expressible as the square of a wave function corresponding to one arrangement of spin orientations. The rather nearly complete cancellation, at low bombarding energies, of $s$ and $p$ waves to give a markedly reduced intensity at some angle seems to indicate that the intensity arises preponderantly as the square of one wave function, or as the superposition of the squares of several wave functions but with similar angular properties. At some higher bombarding energies no low dip in the intensity appears at any angle, and there is thus no evidence that one wave function or type of wave function predominates. Whether there be one or several components of the intensity distribution, it would be expected that it could be expressed as a sum of terms of the form

$$\sin^m\theta_r \cos^n\theta_r,$$

with the exponents $m$ and $n$ going to values not more than twice the highest orbital angular momentum quantum number involved in the outgoing waves. With five observed values of the intensity, corresponding to the five angles of observation, one has only five values of a continuously varying function with which to determine the arbitrary parameters in terms of which it may be expressed. It would be hoped that there would be fewer than five terms of the above-mentioned form so as to allow some verification of the parameter determination. This does not seem to be the case, so the best one can do is to try to fit the five data with five parameters. This process ordinarily involves the use of fifth-order determinants and correspondingly lengthy computation. The computations are simpler if one limits $m$ to zero and analyzes the intensity in powers of $x=\cos\theta_r$ from the zero power to the fourth power, inclusive. This is done

TABLE IV. Coefficients in some of the expansions in angle functions.

| $E$/Mev Short range | $A_0$ ($\alpha_0$) | $A_1$ ($\alpha_1$) | $A_2$ ($\alpha_2$) | $A_3$ ($\alpha_3$) | $A_4$ ($\alpha_4$) |
|---|---|---|---|---|---|
| 0.65 | 0.61 | −1.11 | 0.74 | 0.68 | −0.29 |
| | (0.28) | (−0.71) | (0.33) | (0.27) | (−0.07) |
| 1.07 | 14.7 | −13.1 | −8.6 | 9.1 | 5.6 |
| 1.07 | (12.9) | (−7.6) | (−2.5) | (3.6) | (1.3) |
| 1.785 | 46.9 | 5.4 | −59.7 | −23.7 | 38.1 |
| 3.05 | 49.7 | 14.7 | −52.0 | −21.4 | 5.7 |
| Long range | | | | | |
| 1.07 | 3.1 | 4.1 | 1.7 | −4.0 | −3.1 |
| | (3.1) | (1.7) | (−0.6) | (−1.6) | (−0.7) |
| 1.785 | 10.6 | −3.3 | 8.6 | −2.3 | 5.7 |
| 3.05 | 41.0 | 40.2 | 10.8 | −56.4 | −31.7 |

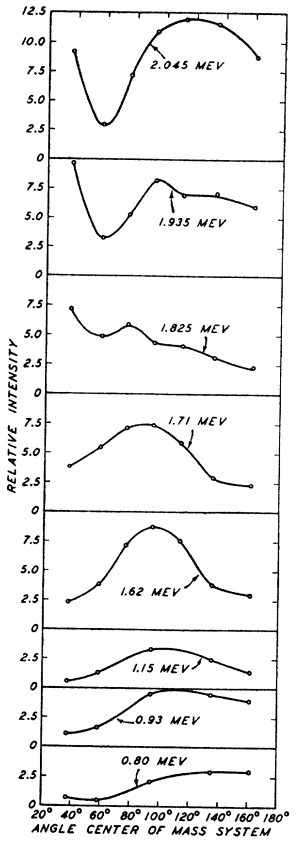


FIG. 5. Angular distributions of the short-range protons observed with a thin oxide target on steel.

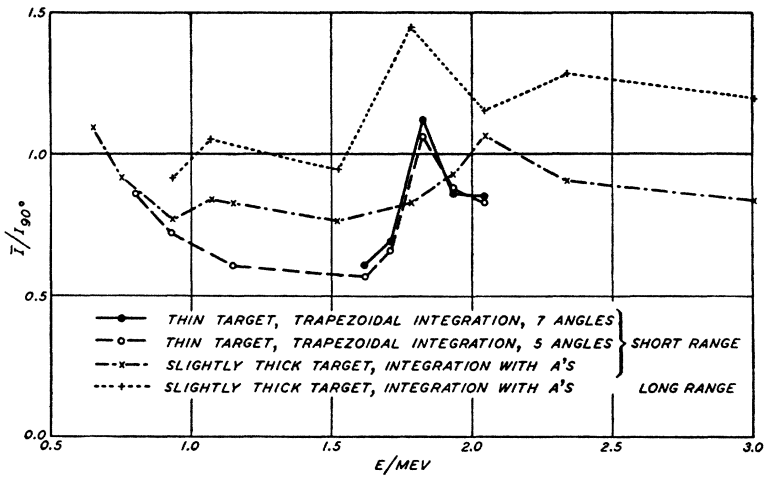


FIG. 6. Average intensity over the entire sphere, relative to the intensity at 90°.

by means of an expansion by products:[8] the five angles at which observations are made are numbered from $n=0$ to 4, and the intensity is written

$$I(x)=a_0+a_1(x-x_1)+a_2(x-x_1)(x-x_2)+\cdots$$

to five terms. Then the $a_n$ are determined by putting $a_0=I(x_1)$, $a_1=(I(x_2)-I(x_1))/(x_2-x_1)$, etc. The terms so obtained are combined to give an expansion in powers of $x$, and this has in some cases been rearranged to give coefficients of the normalized Legendre functions:

$$I(x)=\sum_{k=0}^{4}A_kx^k=\sum_{l=0}^{4}\alpha_lP_l^0(x),$$

with the $P_l^0$'s of course equal to $2^{-\frac{1}{2}}$, $(3/2)^{\frac{1}{2}}x$, $(5/2)^{\frac{1}{2}}(3x^2-1)/2$, $(7/2)^{\frac{1}{2}}(5x^3-3x)/2$, and $(9/2)^{\frac{1}{2}}\times(35x^4-30x^2+3)/8$, respectively. Some typical samples of the results of this analysis are given in Table IV.

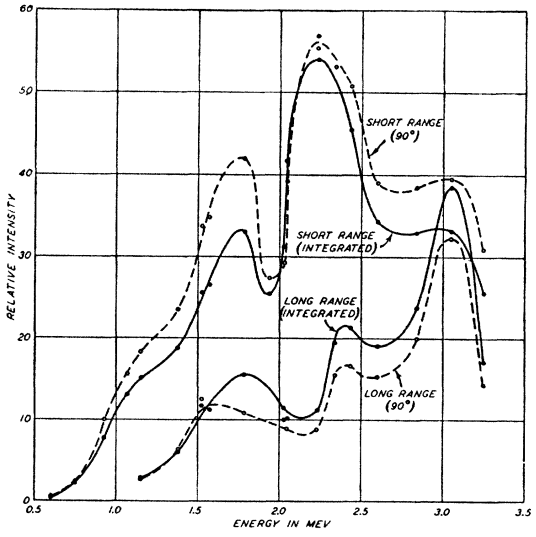


FIG. 7. Excitation curves for the short-range and long-range protons, obtained with slightly thick oxide targets. Both the 90° intensity and the average intensity are shown as functions of bombarding energy.

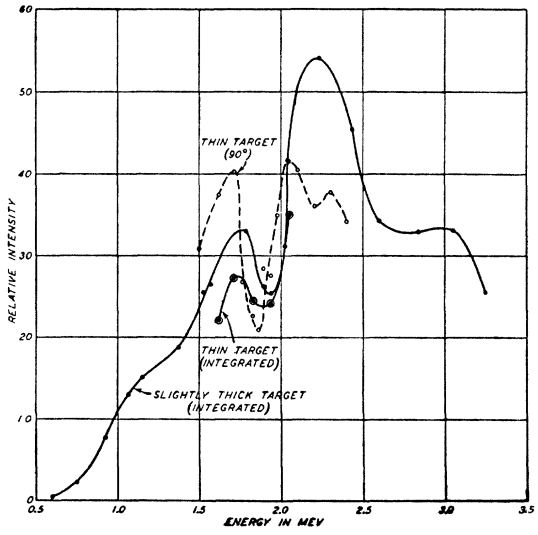


FIG. 8. Excitation curve for the short-range protons, obtained with a thin oxide target on steel. The average intensity curve for the short-range protons from Fig. 7 is repeated here for comparison.

[8] Runge and König, *Numerisches Rechnung* (Julius Springer Verlag, Berlin, 1924), p. 97.

If there were no transitions between incoming deuteron and outgoing proton in which spin and orbital angular momenta were interchanged, then the outgoing waves would have in common with the incoming waves the property of having no component of orbital angular momentum parallel to the axis of incidence, and this is the situation to which our trial analysis in powers of the cosine, or in the $P_l^0$'s, corresponds. One would expect the terms with higher values of $l$ to have extremely small coefficients because of the necessity of penetrating the "centrifugal barrier" (if the process does indeed involve a compound nucleus). That the higher $a$'s and $\alpha$'s do not vanish probably indicates that the analysis should be carried out with a more general expression for the distribution function, including sine terms. This over-simplified analysis on the theoretically untenable hypothesis of very small spin-orbit interaction was tried merely as a preliminary exploration for an unexpected simplicity, so its failure to display convergence is not to be considered in any way disturbing.

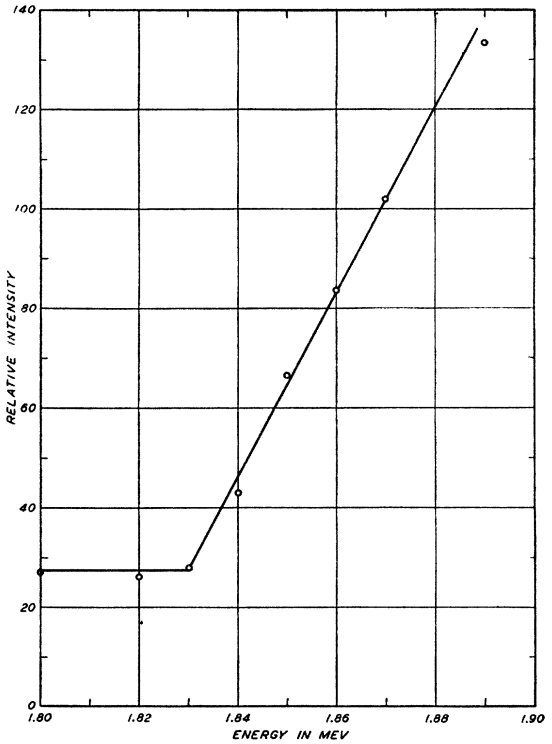


FIG. 9. 90° excitation curve of the competing reaction $O^{16}(d,n)F^{17}$ near its threshold.

### INTEGRATED EXCITATION CURVES

The total yield $Y(E)$ of the reaction at a given energy, integrated over all directions of the product particle, may be obtained fairly reliably by interpolation between the five angles at which observations were made (and even more reliably in the cases where seven observations were made). The extrapolation to 0° and to 180° introduces little uncertainty because very little solid angle is involved near the poles. Several methods are available for carrying out the integration. In the cases where the spherical harmonic analysis was carried out, the most reliable integration is considered to be that over the smooth curve through the observed points provided by this analysis:

$$Y(E)=4\pi\bar{I}=2\pi\int_{-1}^{1}I(x)dx=2\pi\sum_{l=0}^{4}\alpha_l^2$$
$$=4\pi(A_0+A_2/3+A_4/5).$$

The demands on accuracy are not so great but that a simple trapezoidal integration may be considered about as satisfactory, and this has been used in cases where the spherical harmonic analysis was not carried out. In the formula used,

$$4\bar{I}=(y_1-y_2)(1-x_1)^2/(x_1-x_2)+y_1(2-x_1-x_2)$$
$$+y_2(x_1-x_3)+\cdots+y_5(x_4+x_4+2)$$
$$+(y_5-y_4)(x_5+1)^2/(x_4-x_5),$$

the first and last terms represent the difference between a linear and a leveled-off extrapolation to the poles and are practically negligible. The results of these calculations of total yield by integration of the intensity over the angles are shown in Fig. 6. The quantity plotted is the average intensity, $\bar{I}$, divided by the intensity at 90°. It is seen that the average intensity is at some energies greater than the intensity at 90°, and at some energies less. The ratio is a convenient quantity because it is a correction factor converting a ninety-degree excitation curve into an integrated excitation curve. At a few energies, observations were interpolated at two additional angles (Table II), and one sees in Fig. 6 that the average intensity obtained by use of all seven angles differs very little from that computed ignoring the extra angles, a fact which gives

confidence in the results obtained from observations at only five angles. One also notes that the peak in the ratio for the short-range curve with a thin target is sharper and lies at about 200-kev lower bombarding energy than the corresponding peak obtained with a thicker target.

As mentioned above, an excitation curve is most reliable if readings are taken consecutively at one angle and a succession of energies. For this reason ninety-degree excitation curves have been observed, as has been customary in investigations not concerned with angular distributions. The ninety-degree excitation curve for the long-range and the short range protons are shown with dotted lines in Fig. 7. Quite interesting structure appears, especially the peak in the short-range curve in the neighborhood of 1.8 Mev. Observations were made with the thin target at more closely-spaced energies near this peak, and in Fig. 8 a separate excitation curve is shown for these. In Figs. 7 and 8 are also shown, in solid lines, the more significant curves representing the average intensity or integrated excitation curve, obtained from the ninety-degree results and from the ratios plotted (with somewhat dubious interpolation at the higher energies) in Fig. 6. It is gratifying to note that the presumably more significant integrated excitation curves display a similarity between the resonances in the short-range and long-range results that was not apparent in the ninety-degree curves.

### THE COMPETING REACTION $O^{16}(d,n)F^{17}$

The dip in the excitation curve beyond the peak at about 1.8 Mev comes near the threshold of the competing $(d,n)$ reaction. This reaction was first observed, through the resulting positron activity, by Newson,[9] who found the threshold at about 2 Mev (perhaps 100 kev lower according to newer range-energy information). In order to establish this threshold on the same energy scale used for the $(d,p)$ reaction and thus have a direct comparison with the position of the dip in the excitation curve observations have been made on the neutrons emitted at about 90° to the deuteron beam, from a slightly thick target on steel. A boron-lined ionization chamber was used, surrounded by about 5 cm of paraffin. The neutron intensity thus detected, as a function of bombarding energy, is shown in Fig. 9. The threshold thus determined lies at 1.83 Mev, which is indeed very close to the position of the dip in the short-range excitation curve. Incidentally, this gives

$$Q = -1.615 \pm 0.01 \text{ Mev}$$

and the mass of $F^{17}$ as $17.007518 \pm 0.000015$ if we consider our absolute voltage scale[10] to be uncertain by $\frac{1}{2}$ percent. (Here we have taken the deuteron and neutron masses $2.014721 \pm 0.000006$ and $1.008937 \pm 0.000008$).

One is tempted to attribute the peak near 1.7 Mev to the cutting of a cravass in an ascending slope by the competing reaction. However, the nature of the angular distributions seems to be compatible with the assumption that the peak is a resonance. If the resonance levels of the compound nucleus are at all separated, one expects from the dispersion formula that one resonance will have a dominant influence on the angular distribution at energies in the immediate neighborhood of that resonance. Since asymmetry about 90° arises from the interference of the outgoing waves from different compound states, one expects approximate symmetry about 90° when one state is dominant. The curves of Figs. 3 and 4 show a tendency to become more nearly symmetrical about 90° as the energy approaches from below the energy of the peak in the excitation curve, which leads one to believe that this peak is due to a resonance, not simply to $(d,n)$ competition.

The one of us from a neighboring institution wishes to thank Dr. J. A. Flemming and Dr. M. A. Tuve, successive directors, for permitting and encouraging his use of the long-productive experimental facilities of the D.T.M. We express our gratitude also to W. D. Whitehead, Jr., for help in making the observations during the last phase of the work, to Mrs. D. R. Inglis for carrying out most of the computations, and to W. A. Higinbotham of the Federation of American Scientists for consultation concerning a circuit.

[9] H. W. Newson, Phys. Rev. **48**, 790 (1935).

[10] O. A. Hanson and D. L. Benedict, Phys. Rev. **65**, 33 (1944).